**Geomechanics and Engineering**, *Vol. 42, No. 1 (2025) 57-66*
https://doi.org/10.12989/gae.2025.42.1.057


# Analysis on the lateral earth pressure coefficients of soil plugs for large diameter driven piles considering plugging effect

Sumin Song[1a], Junyoung Ko[2b] and Hyunsung Lim*[3]

[1]*Department of Civil Engineering, National Taiwan University, Taipei, Taiwan*
[2]*Department of Civil Engineering, Chungnam National University, Daejeon, Republic of Korea*
[3]*Hanwha Ocean, Seoul, Republic of Korea*

(*Received November 1, 2024, Revised June 12, 2025, Accepted June 25, 2025*)

**Abstract.** When the installation of large diameter driven pile, the plugging effect is generally caused as the partially plugged condition. In this condition, it is a key issue for design because the inner shaft friction between soil plugs caused by plugging effect and pile's inside surface causes additional bearing capacity of driven piles. Thus, this study suggested a new method for evaluating the inner shaft friction caused by partially plugged condition. The CEL (Coupled- Eulerian-Lagrangian) method was used to simulate the driven pile installation process and proposed the trend of lateral earth pressure coefficient ($K_{plug}$) in soil plugs and the normalized effective soil plug's height. In order to consider drieveability during the hammer driving, each driving energy was separately calculated in each analysis case. Based on parameter studies, it was shown that the plugging effect decreased with increasing the pile diameter, and increased with increasing the pile length, the elastic modulus of soil and the driving energy. It was found that the trend of $K_{plug}$ had almost uniform trends under the different parameters. A simple equation for inner shaft friction at the pile inside was proposed by using the proposed $K_{plug}$.

**Keywords:** CEL method; driveability; large diameter open-ended driven pile; lateral earth pressure coefficient; plugging effect; soil plug

## 1. Introduction

Recently, there has been an increase in the construction of multi-story buildings on relatively soft soil layers due to urban population concentration and city expansion. Soil-structure interaction is also a key factor in offshore construction projects like wind farms, harbor terminals, and grand offshore bridges. To investigate these geomechanics issues, research on soil-structure interaction is widely being conducted through numerical studies (Lim *et al.* 2022, Lim *et al.* 2023, Kim *et al.* 2023, Jeong *et al.* 2024, Ko *et al.* 2024). In such cases, the supporting bedrock is often deep, necessitating pile foundations, and large-diameter piles are increasingly used in construction design. Typically, pile structures are installed via pile driving with open-ended piles. During driving, soil pushed into the open-ended pile causes a plugging effect inside the pile. While it is commonly assumed that the end of pile is completely plugged when the pile is driven into the soil, various studies have shown that this assumption significantly differs from reality. Many researchers have reported that factors affecting the plugging effect include driving energy (Brucy *et al.* 1991, Jeong *et al.* 2015, Ko *et al.* 2016), pile diameter, pile length (Beringen *et al.* 1979, Klos and Tejchman 1981, Szechy 1959, Kishida 1967, Matsumoto and Takei 1991), and soil condition (Paik and Salgado 2003, Ko *et al.* 2022).

In order to analyze the existing plugging effect, many field tests and laboratory tests (Brucy *et al.* 1991, Paik and Lee 1993, Paik *et al.* 2003) have been carried out about the bearing capacity of piles. In the case of large diameter piles, however, there is difficult to carry out field tests due to economic and time problems despite of widely used in construction sites. In this study, the plugging effect generated after construction was investigated by simulation of actual pile construction using CEL (Coupled Eulerian-Lagrangian) method, one of the large deformational numerical methods. The CEL method has been used by many researchers to investigate the impact of shaft fracture on TBM tunnels, and to analyze the plugging effect on the pile. (Qiu *et al.* 2011, Kim and Jeong 2014, Lee *et al.* 2017, Ko *et al.* 2016).

The purpose of this study is to analyze the resistance mechanism by soil plugs and develop an inner shaft friction equation considering the plugging effect of sandy soil using the CEL method. The numerical analysis results were compared with field test results for validation. Parameter analyses were conducted to investigate the plugging effect with different pile diameters, pile lengths, soil conditions, and driving energies. Additionally, the lateral earth pressure coefficient generated within the soil plug due to the plugging effect was analyzed, and the equation for bearing resistance force, considering the plugging effect, was developed and discussed.

*Corresponding author, Ph,D., Manager
E-mail: hslim@hanwha.com
[a]Ph.D., Post-doctoral
E-mail: ssm9780@ntu.edu.tw
[b]Associate Professor
E-mail: jyko@cnu.ac.kr



ISSN: 2005-307X (Print), 2092-6219 (Online)

## 2. Plugging effect of large diameter open-ended piles

There are three conditions in the plugged condition. A fully plugged condition is completely plugged and behaves like a closed pile. On the other hand, an unplugged condition is fully open and easy to generate soil plugs. According to White *et al.* (2005) and Ko *et al*. (2016), open-ended driven piles have the characteristics as partially plugged when the pile is driven into the soil (Fig. 1). The open plugged condition or fully plugged condition is very easy to calculate the bearing capacity at the pile tip, but a partially plugged condition is difficult to design because it requires much consideration of several influencing conditions such as pile diameter, pile length, and driving energy during the pile driving. Especially, the influence condition is significantly complicated in the case of a large diameter open-ended driven pile. Although many previous studies found that it has a sensitive and complicated behavior caused by the influence conditions, previous studies did not consider appropriate driving energy changes with the pile's physical size and soil condition.

In other words, taking into account estimating the driving energy for each case, the criteria is called BPM, which is driveability. In the in-situ field, BPM is determined whether a predetermined bearing capacity has been reached through the number of a blow per unit length of the pile (Blow Per Meter, BPM) at the time of pile driving. If the number of strikes per unit penetration is large, economic efficiency in terms of time and cost is low and the pile is damaged due to unreasonable impact on the pile. In general, the concrete pile has the limitation of BPM as 200/m and the steel pile has 500/m. If a hammer with a relatively small load is used in comparison with the ground and pile, the bearing capacity is less than the designed bearing capacity because the target penetration depth is not penetrated. Therefore, in this study, in order to establish a criterion for quantifying driving energy to pile size, driveability (BPM) was used for each analysis case.

When the design of large open-ended driven steel piles, conservative design is primarily used up to now because the pile tip's resistance mechanism is complicated and there are no clear design criteria. The existing design equation is a design technique based on SPT and CPT, the site exploration result values are high in general higher strength soil. Therefore, the pile tip bearing capacity predicted through the design code becomes much larger than the actual pile tip bearing capacity. For this reason, the bearing capacity of the pile tip can be predicted excessively when a large diameter pile is installed in a high degree of soil. Therefore, this study developed a pile base bearing capacity design method considering the plugging effect by using the lateral earth pressure coefficient which is not affected by the in-situ results. And the lateral earth pressure coefficient ($K$)can be calculated as

$$K = \frac{\sigma_h}{\sigma_v} \tag{1}$$

where, $K$ is the lateral earth pressure coefficient, $\sigma_h$ is the horizontal earth pressure and $\sigma_v$ is the vertical earth pressure. According to Ko and Jeong (2015) and Paikowsky

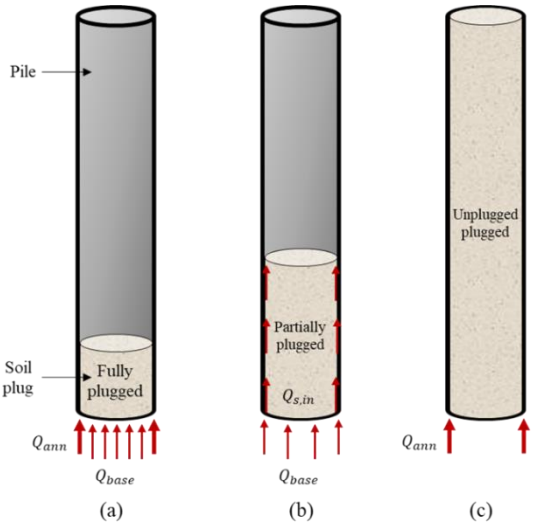


Fig. 1 Three conditions of plugging effect after pile driving: (a) fully plugged condition, (b) partially plugged condition and (c) open plugged condition

(1990), they suggested that not all of soil plug's height, only certain height of it generates the inner shaft friction as following Eq. (2)

$$SPI = \frac{L_{stress}}{L_{plug}} \times 100(\%) \tag{2}$$

where, $L_{stress}$ is the height of soil plug which occurs the inner shaft friction, $L_{plug}$ is the total soil plug after pile driving.

## 3. Coupled Eulerian-Lagraingian (CEL) analysis

### *3.1 CEL modeling*

The plugging effect can be occurred during pile driving, it is essential to simulate driving impact and soil plug generation. This study utilized the Coupled Eulerian-Lagrangian (CEL) method in ABAQUS/Explicit (2013) to make modelling of installation process of open-ended driven piles. A 3D Finite Element (FE) mesh model is illustrated in Fig. 2. Exploiting symmetry in the modelling, only a quarter of the domain was used with symmetric boundary conditions imposed on two planes to ensure zero flow velocity normal to these planes. The base of the FE model was constrained to prevent vertical and horizontal flow, and radial flows were allowed at the curved face representing the far-field boundary. The domain dimensions included a width of 10 times the pile diameter ($D$) and a height twice the pile length ($L$), considering the reflection of driving energy.

As following to the CEL method, the piles were modelled within the Lagrangian domain, while the soil was modelled in the Eulerian domain. The soil was divided into a double layer: a soil layer and a void layer. This setup accounted for the soil being displaced into the empty elements (inside the pile) during penetration steps. The soil

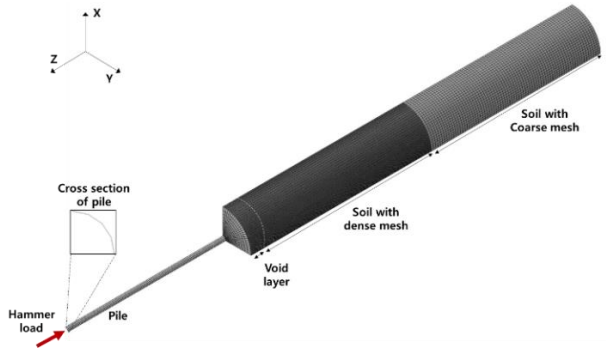


Fig. 2 Geometry and finite element for soil and pile modeling

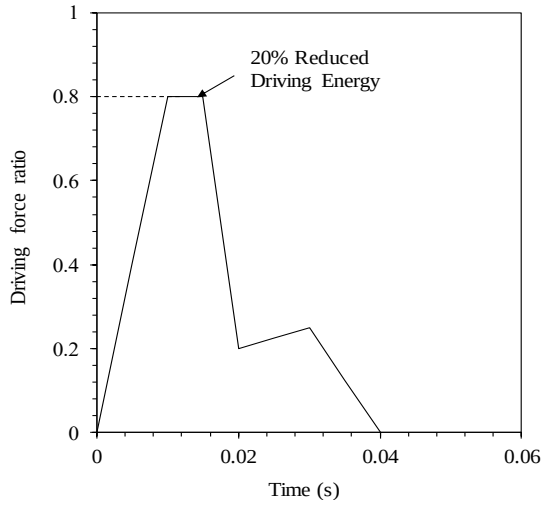


Fig. 3 Driving load curve of one hammer blow (Goble *et al.* 1980)

layer had defined strength and stiffness values, whereas the void layer did not. The soil mesh domains used 8-node Eulerian brick elements (EC3D8R), and the pile mesh domains used 8-node Lagrangian brick elements (C3D8R).

The interface between the pile and soil was modelled using Coulomb's frictional model, reflecting the general contact conditions specified in ABAQUS/Explicit (2013).

$$\tau_c = \mu \cdot p \tag{3}$$

where, $\tau_c$ is the shear force, $\mu$ is the friction coefficient, $p$ is the contact force.

The specified initial stress state should align with calculations based on the self-weight of the material and the geometries involved. Therefore, a geostatic stress condition is imposed in a predefined step to account for the soil weight. Following this initial step, a load is applied to simulate the pile driving process by exerting a driving load at the top of the pile. Under the driving load condition, the loading time for one hammer blow from the driving hammer is illustrated in Fig. 3. These driving loads are applied repeatedly until the target penetration depth is achieved. The piles were driven with a driving cycle of 0.04 seconds, as studied by Goble *et al*. (1980).

### *3.2 Mesh studies*

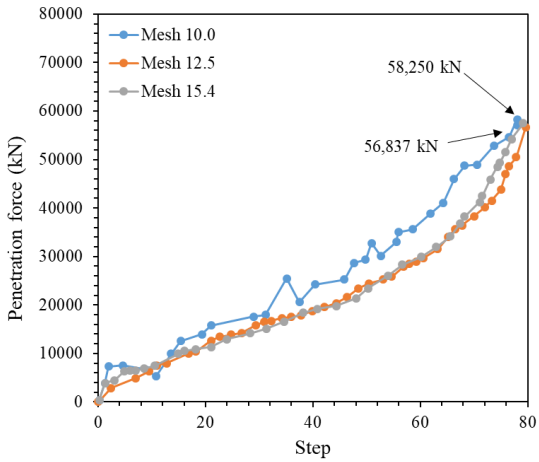


Fig. 4 Results of mesh study

Table 1 Input parameters of mesh study (Gwangyang site)

| Type | Model | $\gamma_t$ (kN/m$^3$) | $E$ (MPa) | $\phi$ *(deg)* | *Poisson's ratio, v* |
|---|---|---|---|---|---|
| Pile ($D$ = 2 m, $L$ = 45 m) | Linear elastic | 75 | 210,000 | - | 0.2 |
| Sand | Mohr-coulomb | 18 | 13.5 | 32 | 0.3 |

A representative analysis model is as $D$ = 2.0 m and $L$ = 45 m of driven large diameter condition, it penetrated homogeneous sandy soil and the input parameters were noted in Table 1. Mesh studies were performed for securing the analysis precision and computational time duration efficiency. Table 2 summarized the mesh studies' results. According to the mesh size ratio decreased from 15.4 to 10.0, the mesh density increased from the 10.0 to 15.4. In addition, increased the mesh density caused to increase the computation time dramatically.

The stress-penetration depth curves were presented with three different mesh density cases in Fig. 4. Although the different analysis times were spent with three cases, two results (Mesh 12.5 and 15.4) showed similar penetration force at the end of step. Therefore, Mesh 12.5 seems to be the most efficiency computation mesh size ratio, the mesh size 15.4 was chosen to main analysis.

### *3.3 Driving energy considering driveability (BPM)*

According to existing studies, the driving energy has been reported that it is significantly important factor for plugging effect, so, this study had to calculate uniform energy ratio to simulate in-situ installation for all of analysis cases. In this study, the BPM (Blow per meter) was utilized to control driving energy for each case, GRL-WEAP program was used in this study to calculate the BPM (Pile dynamics Inc., 2010).

The driveability is calculated based on wave equation analysis when the pile was driven into the soil until the target soil depth. This study assumed that the BPM 500 is the minimum required driving energy when the open-ended steel pile is penetrated the soil.

Table 2 Results of mesh study

| | Min. size of mesh | $D$ / mesh size | Number of Elements | Computation Time ($hr$) | Ultimate penetration force, $P_u$ (kN) |
|---|---|---|---|---|---|
| Mesh 15.4 | 0.13 | 15.4 | 4,751,388 | 148 | 56,398 |
| Mesh 12.5 | 0.16. | 12.5 | 2,527,322 | 24 | 56,837 |
| Mesh 10.0 | 0.2 | 10.0 | 1,320,084 | 9 | 58,250 |

Table 3 Comparison of plug length with field data and numerical simulation

| | $L_{plug}$ | | |
|---|---|---|---|
| | Measured data (Ko and Jeong 2015) | Previous study (Ko *et al.* 2016) | This study |
| TP-1 | 1.30 | 1.80 | 1.82 |
| TP-2 | 2.00 | 1.94 | 1.99 |
| TP-3 | 2.30 | 1.84 | 1.85 |

Table 4 Validation of SPI with field data and analysis results

| | *SPI (%)* | | |
|---|---|---|---|
| | Measured data (Ko and Jeong 2015) | Previous study (Ko *et al.* 2016) | This study |
| TP-1 | 34.4 | 40.0 | 41.2 |
| TP-2 | 23.1 | 22.6 | 20.3 |
| TP-3 | 17.4 | 13.1 | 14.3 |

Commonly, BPM increased as penetration depth increases when the pile is driven into the soil layer. Finally, when the pile arrived the target penetration depth, at that time BPM is 500. As a result, that the driving energy was selected.

In this analysis, the soil layer is modelled as the homogeneous sand, the inter friction angle ($\phi$) is varied as 26, 34 and 39.5°, and the unit weight of soil is fixed to 18 kN/m3. Driving efficiency was 0.8 recommended by GRL-WEAP manual (Pile dynamics Inc., 2010). Connections of pile were not considered in the pile modelling. One of the standard materials of pile, SKK590 was chosen for this analysis, and it has the allowed stress of 440 MPa.

### *3.4 Validation of CEL analysis with field test results*

The CEL modelling of this study validated to an in-situ test result of the plugging effect (Ko and Jeong 2015). Tables 3 and 4 showed the result of validation, it was shown that this modelling can simulate the results of field testing results relatively.

## 4. Parametric study results and discussions

The cases of parametric study were summarized in Table 5. A series of the CEL analyses on large open-ended piles installed into sandy soils were performed with different

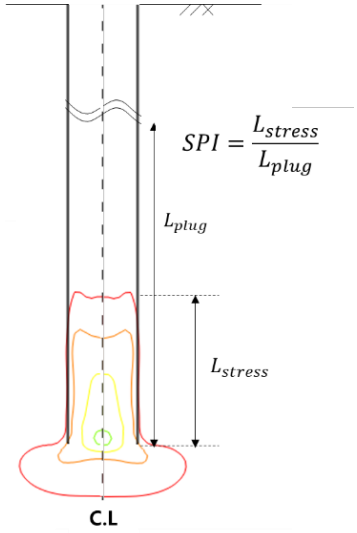


Fig. 5 Results of mesh study

major influence parameters, the pile diameters ($D$), the pile length ($L$), the elastic modulus of sand ($E_s$), and required driving energy considering driveability, BPM ($E_d$).

### *4.1 The behavior of SPI*

Analysis results with different pile diameters summarized radial stress contours of soil plugs in Fig. 6. Radial stress contours of soil plugs were decreased with increasing pile diameters. Note that the method for calculating SPI by using CEL analysis results illustrated in Fig. 5.

The analysis results of SPI with different input parameters were summarized in Fig. 7 based on Figs. 6 and 5. It was found that the SPI with different pile diameters had a constant trend of around 13 % (Figs. 7(a) and 7(b)). According to Ko *et al.* (2016), they showed that SPI tends to decrease with increasing pile diameters from 0.5 – 2 m. Comparing SPI results with varying pile diameters showed different trends in Fig. 8. It is supposed that this difference was caused by the driveability used in this study. This study considered driveability for each analysis condition to change the pile driving energy. So, it means that using adequate pile driving energy can generate the constant amount of SPI after pile driving. In addition, the SPI showed increased trend with increasing the elastic modulus of soil (Figs. 7(c) and 7 (d)) shows the decreasing SPI trend with increasing BPM. Here, it means that the increasing BPM refers to the decreasing pile driving energies, so this trend had similar with previous study result (Ko *et al.* 2016).

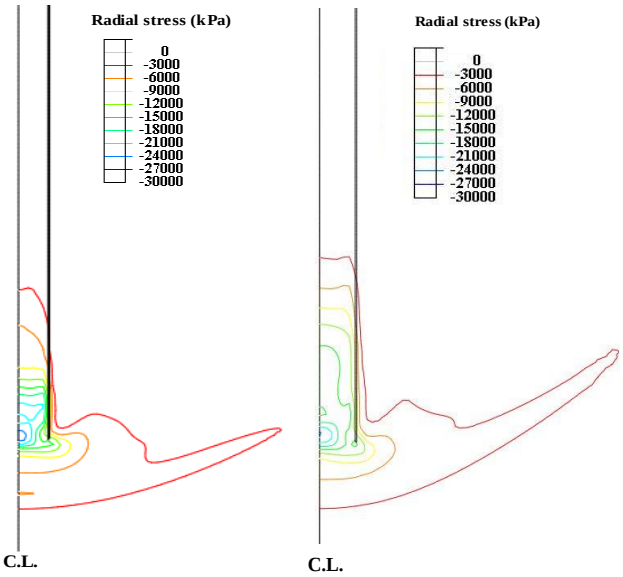


(a) $D$ = 1.5 m (b) $D$ = 2.0 m

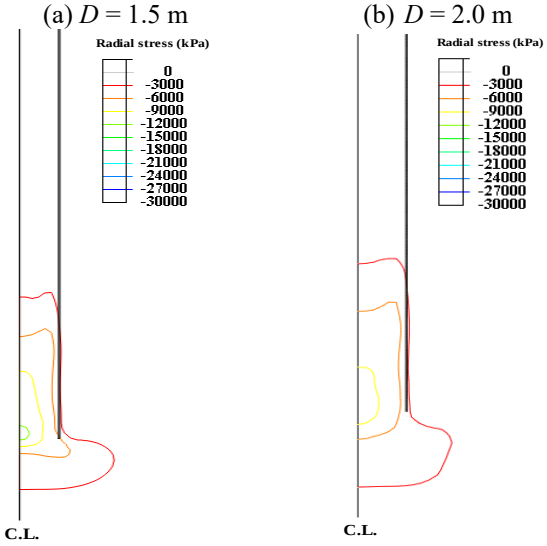


(c) $D$ = 2.5 m (d) $D$ = 3.0 m

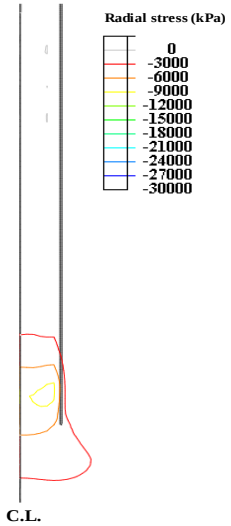


(e) $D$ = 3.5 m

Fig. 6 Typical radial stress contours with varying pile diameters

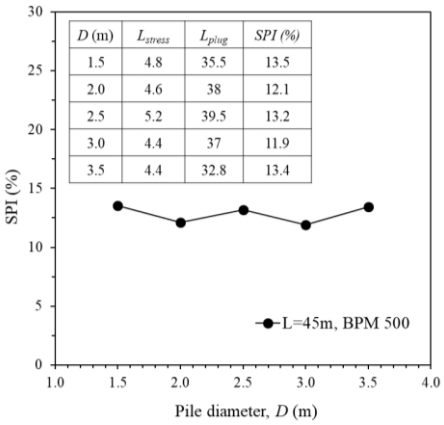


(a) Pile diameters

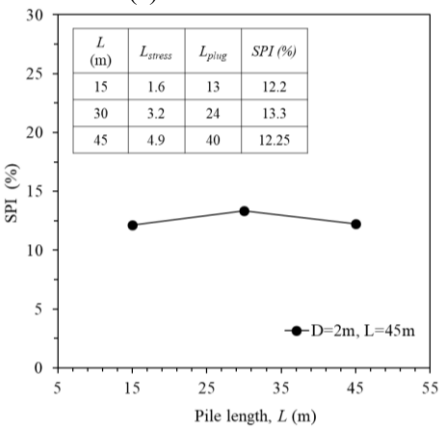


(b) Pile lengths

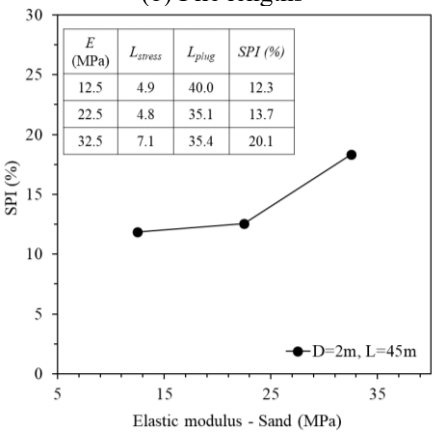


(c) Elastic modulus of sand

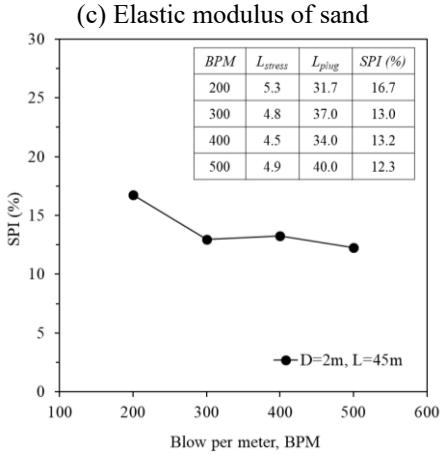


(d) Driveability (BPM)

Fig. 7 SPI with varying influence factors

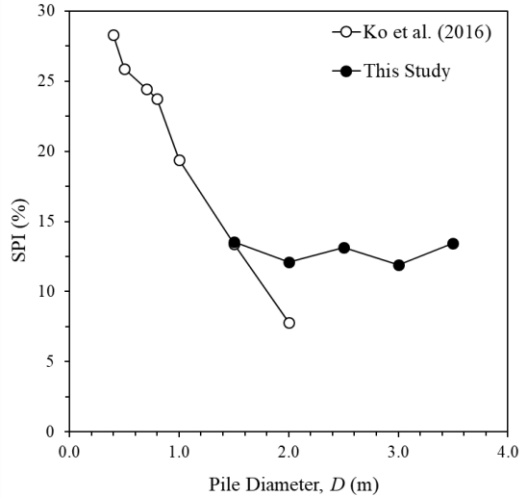


Fig. 8 Comparison of numerical analysis results with existing study (Ko *et al.* 2016)

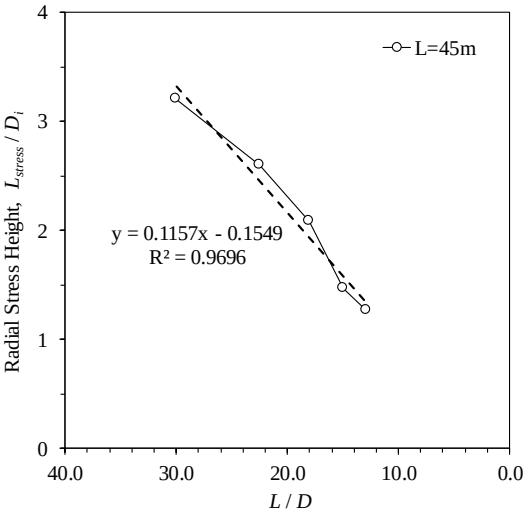


Fig. 9 Normalized height of radial stress in soil plug with varying $L$ / $D$

### *4.2 The height of $L_{stress}$*

Fig. 9 shows the normalized height $L_{stress}$ with varying the pile diameter ($L$ / $D$) under different pile diameter conditions. Although the driveability considered in this study, the normalized height of $L_{stress}$ decreased with increasing of pile diameters. The trend line (Eq. (4)) in Fig. 9 represents the distribution of $L_{stress}$ for piles of various diameters, considering driveability.

$$L_{stress}/D_i = 0.12 \cdot \frac{L}{D} - 0.15 \tag{4}$$

### *4.3 The behavior of lateral earth pressure coefficient ($K_{plug}$) in the soil plug*

The distributions of the lateral earth pressure coefficient ($K_{plug}$) in the soil plug from the pile tip are described in Fig. 10. It was shown that the $K$ of soil at the bottom of pile tips had around 0.5 similar to input K, but the distribution of $K_{plug}$ showed increased until around 2.2 ~ 2.5 then decreased to around 1.5 along the distance from pile tips. This tendency was caused by the results of radial stress contour in soil plugs according to Figs. 5 and 6.

Fig. 11(a) shows the normalized results with pile depths divided by pile diameters, and it was found that combined data showed similar trends of $K_{plug}$. So, the averaged trend curve of $K_{plug}$ with normalized pile depths was calculated in Fig. 11(b) to investigate the trend of distribution.

## 5. Development of inner shaft friction equation for considering plugging effects

### *5.1 Development of inner shaft friction equation for large diameter driven piles with plugging effect*

In this study, the inner shaft friction equation that occurs between the soil plug and the pile was calculated through the distribution trend of $K_{plug}$ calculated through CEL analysis. The horizontal earth pressure coefficient was selected linearly by dividing each section into five sections as shown in Eq. (5). It was assumed that the inner shaft friction only works until the 5 $D_i$ based on the numerical analysis results and $K_{plug}$ occurs consistently as 1.5 from 2.2 $D_i$ to 5 $D_i$.

$$\begin{aligned} K_{plug} &= 0.875x + 0.4 \ (0 \le x \le 0.75), \\ &= 1.875x + (0.75 \le x \le 1.2), \\ &= 2.25 \ (1.2 \le x \le 1.7), \\ &= -1.5x + 4.8 \ (1.7 \le x \le 2.2), \\ &= 1.5 \ (2.2 \le x \le 5.0) \end{aligned} \tag{5}$$

Eq. (4) can be changed as shown in Eq. (6), through which $K_{is}$ expression can be derived as Eq. (7).

$$L_{stress} = D_i(0.12 \cdot \frac{L}{D} - 0.15) \tag{6}$$

$$K_{is} = \frac{1}{L_{stress}} \int_0^{L_{stress}} K_{plug}\, dx \tag{7}$$

where, $K_{is}$ is calculated $K_{plug}$ along the inside shaft of piles, and x is the normalized distance from the pile tip ($L_{stress}$/ $D_i$). White *et al*. (2005) reported that when compacted soil plugs rise into pile inside, it occurs inner shaft friction and end bearing stress which is called the partially plugging effect.

This proposed equation of inner shaft friction is based on the common design methods of shaft friction equation (Eq. (8)). This proposed equation is used to predict the outside shaft resistance equation (Eqs. (9) and (10)).

$$Q_{is} = \int_0^{L_i} f_{is} A_{is} \tag{8}$$

Table 5 Overview of the parametric studies lists

| Parameter | $D$ (m) | $L$ (m) | $E_s$* (MPa) | $\phi$ (deg) | Poisson's ratio, ν | Required Driving energy (kN·m) | Driveability (BPM) |
|---|---|---|---|---|---|---|---|
| Pile diameter ($D$) | 1.5 | 45 | 22.5 | 34 | 0.3 | 441 | 500 |
| | 2.0 | 45 | 22.5 | 34 | 0.3 | 774 | 500 |
| | 2.5 | 45 | 22.5 | 34 | 0.3 | 1,161 | 500 |
| | 3.0 | 45 | 22.5 | 34 | 0.3 | 1,655 | 500 |
| | 3.5 | 45 | 22.5 | 34 | 0.3 | 2,189 | 500 |
| Pile length ($L$) | 2.0 | 15 | 22.5 | 34 | 0.3 | 149 | 500 |
| | 2.0 | 30 | 22.5 | 34 | 0.3 | 589 | 500 |
| | 2.0 | 45 | 22.5 | 34 | 0.3 | 774 | 500 |
| Elastic modulus of Sand ($E_s$) | 2.0 | 45 | 12.5 | 26 | 0.3 | 240 | 500 |
| | 2.0 | 45 | 22.5 | 34 | 0.3 | 774 | 500 |
| | 2.0 | 45 | 32.5 | 39.5 | 0.3 | 1,736 | 500 |
| Required Driving Energy ($E_d$) | 2.0 | 45 | 22.5 | 34 | 0.3 | 774 | 500 |
| | 2.0 | 45 | 22.5 | 43 | 0.3 | 881 | 400 |
| | 2.0 | 45 | 22.5 | 343 | 0.3 | 1,215 | 300 |
| | 2.0 | 45 | 22.5 | 34 | 0.3 | 2,003 | 200 |

* is estimated using the existing previous equation: Es = 500(N+15) (Bowles 2002)

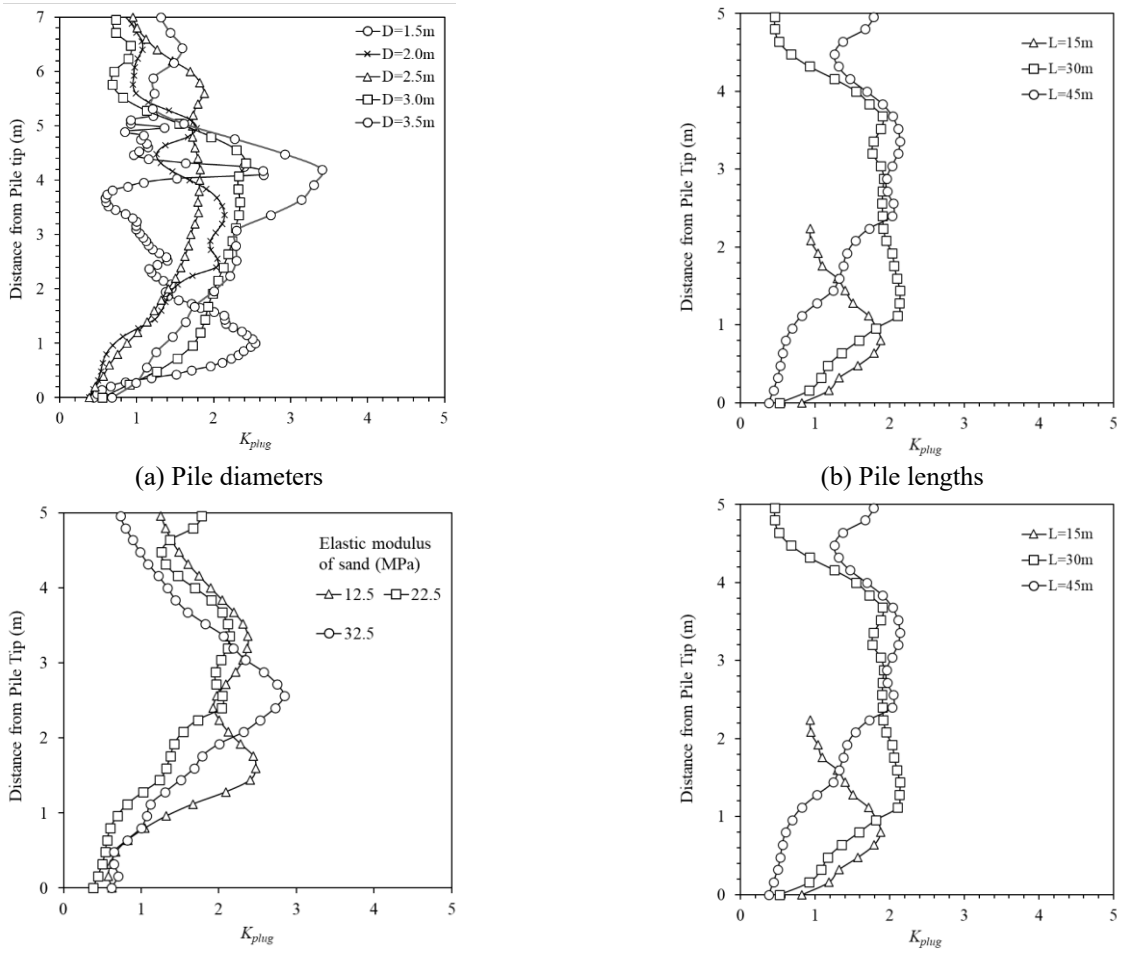


(a) Pile diameters

(b) Pile lengths

(c) Elastic modulus of sand

(d) Driveability (BPM)

Fig. 10 The distribution of lateral earth pressure coefficient

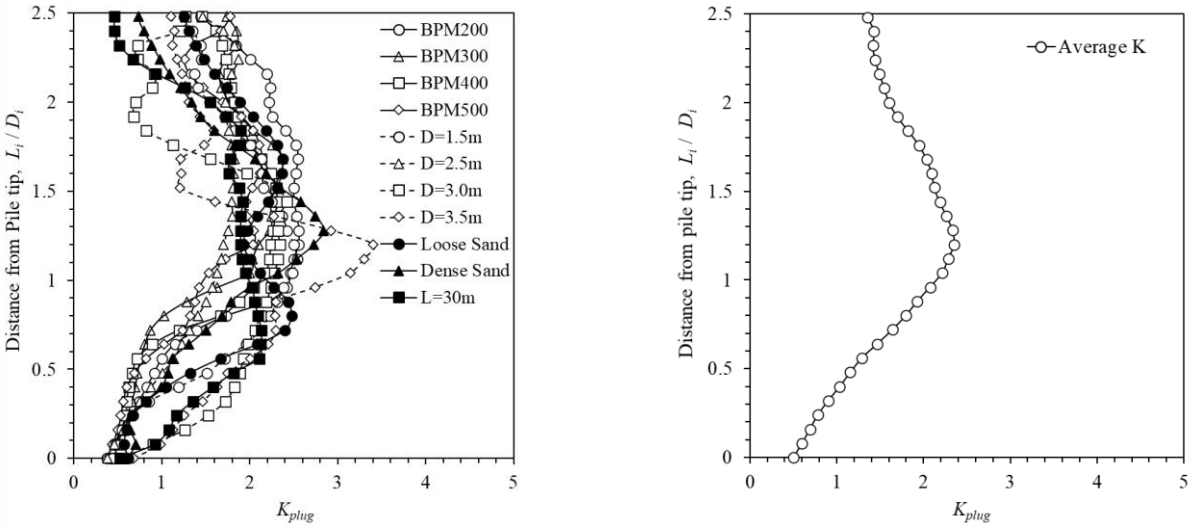


(a) Combined results (b) Averaged results

Fig. 11 The analysis of lateral earth pressure coefficients

$$f_{is} = K_{plug}\tan\delta\sigma'_v \tag{9}$$

$$A_{is} = \pi D_i L_i \tag{10}$$

$$Q_{is} = \frac{1}{x}\int_0^x K dx \tan\delta\sigma'_v \cdot \pi {D_i}^2 (0.12\frac{L}{D} - 0.15) \tag{11}$$

$$\begin{aligned} Q_{tb} &= Q_{ann} + Q_{is} \\ &= N_q \sigma'_v A_{ann} + \frac{1}{x}\int_0^x K dx \tan\delta\sigma'_v \\ &\cdot \pi {D_i}^2 (0.12\frac{L}{D} - 0.15) \end{aligned} \tag{12}$$

where, $Q_{is}$ is the shaft friction in pile shaft, δ is the friction angle between the soil and piles, $\sigma'_v$ is the effective stress of soil, $L$ is the pile length, $D$ is the pile diameter, and $D_i$ is the inner pile diameter.

Reorganizing Eqs. (8) and (9) using Eq. (6) proposed in this study results in Eq. (11).

Total bearing capacity equation ($Q_{tb}$) of open-ended driven pile is Eq. (12) including bearing capacity of an annulus of pile tip and proposed inner shaft friction. The bearing capacity of annulus area is based on the KGS (2015).

In this study, the proposed equation of inner shaft friction was only used by the lateral earth pressure coefficient of soil plug. Since it was hard to predict the unit weight of the soil plugs made by the plugging effect and the friction coefficient (δ) between the pile and the soil.

Fig. 13 shows a summarized process of the proposed equation of inner shaft friction for large diameter driven piles considering plugging effect. This inner shaft friction equation is composed with unit inner shaft friction and inner shaft friction parts. In the unit shaft friction, the $K$ of soil plug is determined by Eq. (7), and inner shaft friction area is determined the $L_{stress}$ by Eq. (6). The annulus bearing capacity equation is followed the design method of

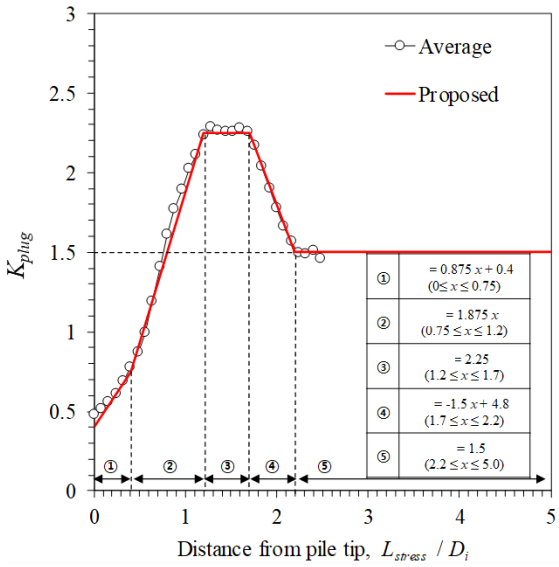


Fig. 12 Proposed the trend of lateral earth pressure coefficient

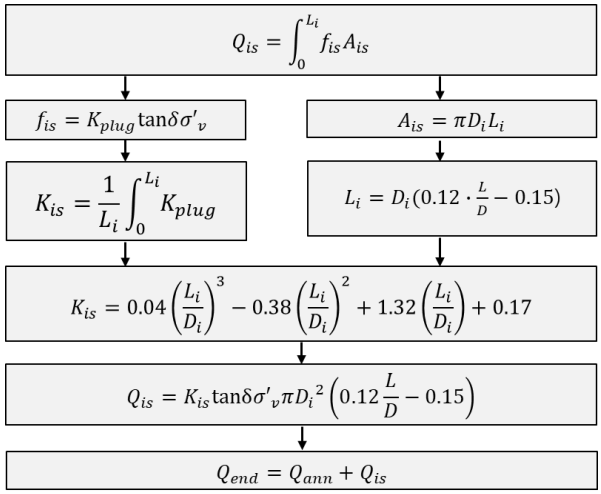


Fig. 13 Proposed inner shaft friction equation for large diameter driven piles

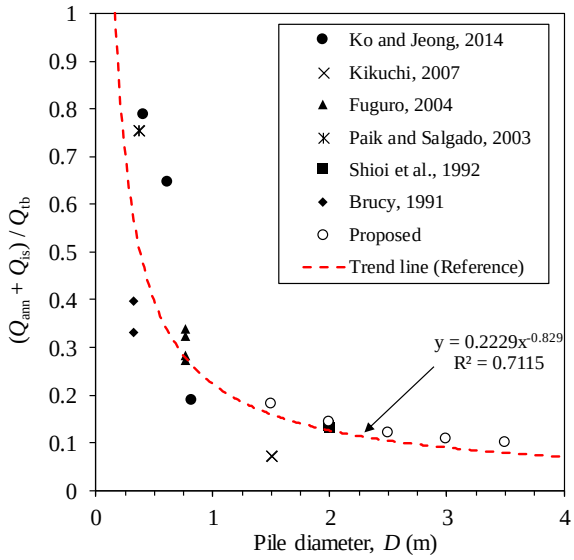


Fig. 14 Proposed inner shaft friction equation for large diameter driven piles

KGS (2015). Finally, the end bearing capacity is combine annuls bearing capacity equation with plugging capacity equation.

### *5.2 Comparison the proposed equation with field test results*

Fig. 14 shows that the ratio of total end bearing capacity to plugging effect bearing capacity with varying pile diameters. It is based on the field load test results (Table 6) and numerical analysis results of this study. Fig. 14 also proposed the trend line of an actual end bearing capacity with the plugging effect. It was found that large diameter piles had a much lower bearing capacity ratio than small and medium diameter piles. It is a reduction in end bearing capacity ratio from 40% ($D$ = 0.508 m) to 10% ($D$ = 2.0 m). Ratio of plugging effect bearing capacity of this proposed curve can be changed dependent on the influencing factors i.e., driving energy and soil condition.

## 5. Conclusions

The main purpose of this study is to propose a bearing capacity equation based on the results obtained by simulating a large diameter open-ended driven pile with numerical analysis (CEL method). The results of the CEL method were verified and the parametric study was conducted. The following conclusions could be drawn from the present study:

• As a result of applying hanger energy to large diameter pile considering driveability, it was confirmed that the plugging effect is also observed in large diameter piles.

• The plugging effect was analyzed as the height at which $L_{stress}$ occurred. The height of the soil plug was smaller than that of small diameter pile considering the same driveability. Also, the longer the pile length, the harder the soil condition, and the higher the driving energy, the higher the $L_{stress}$.

• The lateral earth pressure coefficient - $L_{stress}$ graphs obtained through the analysis of the influence factors showed a constant tendency. The lateral earth pressure coefficient distribution of the $L_{stress}$ was proposed by dividing the result of this averaging into 5 sections. This graph showed the tendency of the lateral earth pressure coefficient to vary depending on the height of the soil plug and affects the radial stress of the soil plug.

• The bearing capacity equation is proposed using the lateral earth pressure coefficient distribution and the $L$ / $D$ - $L_{stress}$ distribution. The verification results confirm that the measured values are well predicted in the large-diameter pile case.

## Acknowledgements

This work was supported by the National Research Foundation of Korea (NRF) grant funded by the Korean government (MSIT) (No. NRF-2022R1C1C1011477).

## References

ABAQUS. (2013), ABAQUS user's and theory manuals (Version 6.13). Rhode Island: Hibbitt, Karlsson & Sorensen, Inc.

Beringen, F.I., Windle, D. and Van Hooydonk, W.R. (1979), "Results of loading tests on driven piles in sand", *Proceedings of the Conference on Recent Development in the Design and Construction of Piles*, ICE, London, 21-22.

Bowles, J.E. (2002), Foundation analysis and design. New York, USA: McGraw-Hill.

Brucy, F., Meunier, J. and Nauroy, J.K. (1991), "Behavior of pile plug in sandy soils during and after driving", *Proceedings of the 23rd Annual Offshore Technology Conference*, Houston, 1. https://doi.org/10.4043/6514-MS.

Goble, G.G., Raushe, F.R. and Likins, G.E. (1980), "The analysis of pile driving-a state-of-the-art", *Proceedings of the International Seminar on the Application of Stress-Wave Theory on Piles*, Stockholm, Sweden.

Jeong, S.S., Ko, J.Y., Song, S. and Kim, J. (2024), "The behaviors of a Korean weathered soil under monotonic loadings", *Geomech. Eng.*, **38**(2), 157-164. https://doi.org/10.12989/gae.2024.38.2.157.

Jeong, S.S., Ko, J.Y., Won, J.O. and Lee, K.W. (2015), "Bearing capacity analysis of open-ended piles considering the degree of soil plugging", *Soils Found.*, **55**(5), 1001-1014. https://doi.org/10.1016/j.sandf.2015.06.007.

Kim, Y.H. and Jeong, S.S. (2014), "Analysis of dynamically penetrating anchor based on coupled Eulerian-Lagrangian (CEL) methods", *J. Korean Soc. Civil Engineers*, **34**(3), 895-906. https://doi.org/10.12652/Ksce.2014.34.3.0895.

Kishida, H. (1967), "The ultimate bearing capacity of pipe piles in sand", *Proceedings of the 3rd Asian Regional Conference on Soil Mechanics and Foundation Engineering*, Tokyo, Japan, 1.

Kim, J., Ko, J.Y. and Kim, D. (2023), "Analysis on inclined or rounded tip piles using 3D printing technology and FE analysis", *Geomech. Eng.*, **33**(1), 91-99. https://doi.org/10.12989/gae.2023.33.1.091.

Klos, J. and Tejchman, A. (1981), "Bearing capacity calculation for pipe piles", *Proceedings of the 10th International Conference on Soil Mechanics and Foundation Engineering*, Stockholm, Sweden, 2.

Ko, J., Cho, J. and Jeong, S. (2018), "Analysis of load sharing characteristics for a piled raft foundation", *Geomech. Eng*., **16**(4), 449-461. https://doi.org/10.12989/gae.2018.16.4.449.

Ko, J.Y. and Jeong, S.S. (2015), "Plugging effect of open-ended piles in sandy soil", *Can. Geotech. J*., **52**(5), 535-547. https://doi.org/10.1139/cgj-2014-0041.

Ko, J.Y., Jeong, S.S. and Lee, J.K. (2016), "Large deformation FE analysis of driven steel pipe piles with soil plugging", *Comput. Geotech*., **71**, 82-97. https://doi.org/10.1016/j.compgeo.2015.08.005.

Ko, J.Y., Jeong, S.S. and Seo, H.Y. (2022), "Effect of soil condition on the coefficient of lateral earth pressure inside an open-ended pipe pile", *Geomech. Eng*., **31**(2), 209-222. https://doi.org/10.12989/gae.2022.31.2.209.

Ko, J.Y., Lim, H.S., Seo, S.H. and Chung, M.K. (2024), "Assessment of pull-out behavior of tunnel-type anchorages under various joint conditions", *Geomech. Eng.*, **36**(1), 71-81. https://doi.org/10.12989/gae.2024.36.1.071.

Lee, S.Y., Kim, D.H. and Jeong, S.S. (2017), "A study on the excavation damage zone (EDZ) under TBM advancement based on large deformation technique (coupled Eulerian-Lagrangian)", *J. Korean Geotech. Soc*., **32**(12), 5-13. https://doi.org/10.7843/kgs.2016.32.12.5.

Lim, H.S., Park, J.J., Kim, J.H. and Ko, J.Y. (2023), "Numerical study on stability and deformation of retaining wall according to groundwater drawdown", *Geomech. Eng*., **33**(2), 195-202. https://doi.org/10.12989/gae.2023.33.2.195.

Lim, H.S., Seo, S.H., Ko, J.Y. and Chung, M.K. (2022), "Influence of geometric factors on pull-out resistance of gravity-type anchorage for suspension bridge", *Geomech. Eng*., **31**(6), 573-582. https://doi.org/10.12989/gae.2022.31.6.573.

Matsumoto, T. and Takei, M. (1991), "Effects of soil plug on behavior of driven pipe piles", *Soils Found.*, **31**(2), 14-34. https://doi.org/10.3208/sandf1972.31.2_14.

Paik, K.H. and Lee, R. (1993), "Behavior of soil plugs in open-ended model piles driven into sands", *Mar. Georesour. Geotech.*, **11**(4), 353-373. https://doi.org/10.1080/10641199309379929.

Paik, K.H. and Salgado, R. (2003), "Estimation of active earth pressure against rigid retaining walls considering arching effects", *Géotechnique*, **53**(7), 643-653. https://doi.org/10.1061/(ASCE)GM.1943-5622.0001865.

Paik, K.H., Salgado, R., Lee, J.H. and Kim, B.J. (2003), "Behavior of open-and closed-ended piles driven into sands", *J. Geotech. Geoenviron. Eng*., **129**(4), 296-306. https://doi.org/10.1061/(ASCE)1090-241(2003)129:4(296).

Pile Dynamics Inc. (2010), GRLWEAP: Wave equation analysis of pile driving, procedure and models manual. Cleveland.

Qiu, G., Henke, S. and Grabe, J. (2011), "Application of a coupled Eulerian-Lagrangian approach on geomechanical problems involving large deformations", *Comput. Geotech*., **38**, 30-39. https://doi.org/10.1016/j.compgeo.2010.09.002.

Shioi, Y., Yoshida, O., Meta, T. and Homma, H. (1992), Estimation of bearing capacity of steel pipe pile by static loading test and stress-wave theory (Trans-Tokyo bay highway), (Ed., F.B.J. Barends), Application of stress-wave theory to piles (1st Ed.). London, UK.

Szechy, C.H. (1959), Tests with tubular piles. Acta Technica, Hungarian Academy of Science, **24**, 181-219.

White, D.J., Schneider, J.A. and Lehane, B.M. (2005), "The influence of effective area ratio on shaft friction of displacement piles in sand", *Proceedings of the International Symposium on Frontiers in Offshore Geotechnics (IS-FOG)*, Perth, Australia.